

CHARGE-TRANSFER COMPLEXES FORMED BETWEEN 1-HYDROXYBENZOTRIAZOLE *VERSUS* IODINE AND PICRIC ACID ELECTRON ACCEPTORS: ELECTRONIC, INFRARED AND MORPHOLOGICAL CHARACTERIZATIONS

Hany M. Mohamed*

Department of Chemistry, College of Science, Taif University, P.O. Box 11099, Taif 21944, Saudi Arabia

(Received February 12, 2025; Revised March 16, 2025; Accepted March 18, 2025)

ABSTRACT. A charge-transfer process between an electron-rich and an electron-deficient component creates molecular assemblies, which have several uses in a variety of electronic, optical, sensor, and catalysis fields. Therefore, this study was focused on getting some knowledge about the intermolecular charge transfer complexes between the 1-hydroxybenzotriazole (HBT) with picric acid (PA) and iodine (I₂) as π and σ - acceptors. The charge-transfer interaction of the HBT electron donor and the PA acceptor has been studied in methanol solvent. The resulting data referred to the formation of the new CT-complex with the general formula [(HBT)(PA)]. The 1:1 stoichiometry of the reaction was discussed upon the on elemental analysis and photometric titration. On the other hand, the 1:1 HBT-iodine (I₂) charge-transfer complex has been studied spectrophotometrically in chloroform at room temperature with general formula [(HBT)(I₂)]. The electronic absorption bands of (I₂) are observed at ~ 510 nm. Raman laser spectrum of the brown solid iodine complex has two clear vibration bands at 165 and 113 cm⁻¹ due to I₂ stretching frequency, respectively. The scanning electron microscopy (SEM) and energy dispersive X-ray spectroscopy (EDX) of two HBT charge-transfer complexes were discussed.

KEY WORDS: Benzotriazole, Charge transfer, Electron acceptors, Spectroscopic, Morphology

INTRODUCTION

Benzo-fused azoles are a type of heterocyclic compound of great interest in the field of medicinal chemistry because of their characteristics and uses. Drugs with this heterocycle moiety as the primary component have been used extensively in clinics, such as an anthelmintic for humans [1], and benzoimidazole and its derivatives have been studied for decades [2]. Benzoxadiazole, benzothiazole, and benzotriazole are examples of benzo-condensed azoles with three heteroatoms that have been thoroughly investigated for their wide spectrum of biological activity [3, 4]. Few assessments, though, focused on just one nucleus. Providing an overview of benzotriazole-based systems and their significance in medicinal chemistry is, in fact, the goal of this work. Additionally, benzotriazole (BT) functions as a precursor to radicals or carbanions or as an electron donor. Through a sequence of events, including condensation, addition reactions, and benzotriazolyl-alkylation, it can be readily incorporated into various chemical structures [5-7]. Additionally, several writers have documented employing BT as a synthon to create stable nitrenium ions [8]. A tetrahydroquinoline library was also created using polymer-supported benzotriazoles as catalysts [9]. Since appropriately substituted benzotriazole derivatives can boast the most diverse biological properties, such as plant growth regulator [10-13], choleric [14], antibacterial [15], antiprotozoal [16], antiviral [17], and antiproliferative [18] activity, the pharmaceutical industry is primarily interested in BT.

Applications for charge transfer (CT) complexes include DNA binding, drug receptor binding mechanisms, and antibacterial, antifungal, and antitumor properties [19-21]. This response results

*Corresponding authors. E-mail: hhassanin766@gmail.com

This work is licensed under the Creative Commons Attribution 4.0 International License

from a weak exchange between acceptors and donors [22, 23]. The electrical characteristics of CT complexes have also led to their usage as organic solar cells and organic semiconductors [24]. Two non-covalent interactions—hydrogen bonds and dipole–dipole interactions—have been shown to stabilize the solid CT complex [25, 26]. Donor molecules can be quantified by the creation of deep-colored complexes, which are frequently linked with proton transfer reactions between donors and electron acceptors. These complexes absorb energy in the visible or ultraviolet spectrum [27]. Consequently, the amount of donor medications is calculated using absorption values at maximal absorption wavelengths. The donors are typically compounds containing sulphur or nitrogen atoms that have aromatic rings rich in electrons or free electron pairs [28, 29]. Charge transport complexes using hydrogen have drawn a lot of interest from a variety of disciplines, including solar energy storage and surface chemistry. Numerous biological fields also make use of them [30, 31].

In-depth research has been done on charge-transfer complexes involving various organic species due to their unique interactions that result in the transfer of an electron from the donor to the acceptor [32-35]. To create polyiodide ions with intriguing electrical and solar cell applications, such as I_3^- , I_5^- , I_7^- , and I_9^- , iodine was used as a sigma acceptor in reactions with various organic (aliphatic/aromatic) donors, including amines and crown ethers [36-39]. The intermolecular charge-transfer complexes of picric acid or iodine with 1-hydroxybenzotriazole have not been documented in literature reviews. This study examined the charge-transfer chelation of two distinct acceptors (picric acid and iodine) using 1-hydroxybenzotriazole.

EXPERIMENTAL

Chemicals

Iodine, picric acid, 1-hydroxybenzotriazole, and other chemicals and solvents were obtained from Fluka, Aldrich, and Merck companies and utilized without additional purification.

Instrumentals

A Perkin-Elmer CHN 2400 elemental analyzer was used for the elemental analyses. Jenway 4010 conductivity was used to assess the molar conductance of the HBT and their charge-transfer complexes using 10^{-3} mol/L in DMSO. KBr pellets were used to record IR spectra ($4000\text{--}400\text{ cm}^{-1}$) on a Bruker FT-IR Spectrophotometer, and samples' Raman laser spectra were examined using a 50-mW laser on a Bruker FT-Raman. Using a Jenway 6405 Spectrophotometer and a 1 cm quartz cell, the UV/vis spectra of the reactants and products were acquired in the $200\text{--}800\text{ nm}$ range in chloroform solvent (10^{-4} M). Analytical scanning electron microscopy was used to scan the samples for the Jeol JSM-630LA. The elemental analysis was performed using the Energy-Dispersive X-ray Analysis (EDX) instrument, an optional add-on to the JEOL JSM-6390(LA).

Synthesis of iodine-HBT and PA-HBT solid complexes

The two solid charge-transfer complexes of HBT with σ -acceptors (picric acid, PA) and iodine, I_2 were made by combining 1 mmol (0.136 g) of the HBT donor in 15 mL of chloroform with 1 mmol solution of each acceptor in the same solvent while stirring constantly for approximately an hour at room temperature. At room temperature, the mixtures were allowed to precipitate. The colored complexes (brown and yellow) that formed in the solid state were then filtered, cleaned with a small amount of solvent, and then vacuum-dried on anhydrous calcium chloride.

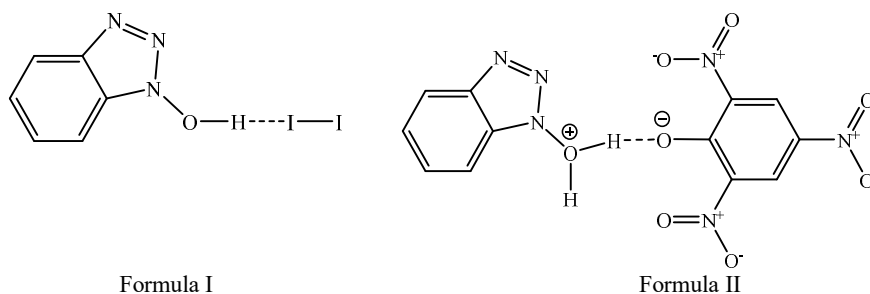
RESULTS AND DISCUSSION

Elemental analysis

The empirical formula for [(HBT)(I₂)] brown complex is C₆H₅ON₃I₂; its percentages are %C, 18.42 (18.53); %H, 1.17 (1.30); and %N, 10.71 (10.80). The empirical formula for [(HBT)(PA)] yellow solid charge-transfer complex is C₁₂H₈O₈N₆; the calculated percentages of C, 39.44 (39.57), H, 2.18 (2.21), and N, 23.01 (23.07) are displayed in parentheses, whereas the experimental data is not. To identify the ideal circumstances for the complexation process, spectrophotometric analysis was used to examine the follow-up of both brown and yellow colors that developed upon the charge-transfer complexes between iodine and picric acid acceptors with HBT donor. The HBT donor functions as a potent electron donor because it has a variety of donating atom types. The proportions of carbon, hydrogen, and nitrogen atoms are in line with the 1:1 molar ratio for HBT-PA and HBT-I₂ between the HBT donor and a few intriguing acceptors, such as iodine and picric acid.

Molar conductance

Starting materials and the resulting HBT charge transfer complexes were measured for conductivity in DMSO at a concentration of 10⁻³ mol/L. The HBT charge-transfer complexes have molar conductivities between 32 and 45 Ω⁻¹cm²mol⁻¹. A slightly electrolytic character was indicated by molar conductance measurements. According to the acid-base theory, this data results from the creation of intermolecular positive and negative dative anions (D⁺—A⁻) [40], see formulas I and II.



Electronic spectra and photometric titration

Figures (1 and 2) display the electronic absorption spectra of the 1:1 CT-complexes that were generated as well as those of the reactants, 1-hydroxybenzotriazole (HBT) (1.0×10⁻⁴ M) with picric acid (PA) and iodine (I₂) (1.0×10⁻⁴ M) in CHCl₃ and CH₃OH. Strong absorption bands can be seen in the spectra of the produced CT-complexes at around 510, and 353 nm for [(HBT)(I₂)], and [(HBT)(PA)], respectively. These bands are absent from the spectra of reactants. It was demonstrated that the HBT-acceptor reactions always had a stoichiometry of 1:1. Both the infrared spectra of the complexes, which show the presence of the bands characteristic for both the HBT and the acceptors, and the elemental analysis data of the isolated solid CT-complexes, as shown in the experimental section, were used to draw this conclusion. Measurements of photometric titration also provide significant support for the 1:1 stoichiometry (Figures 1 and 2).

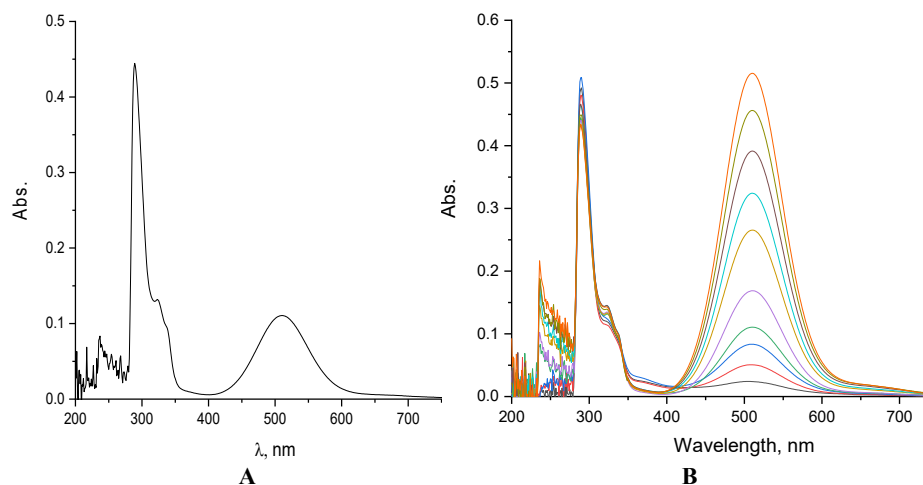


Figure 1. (A): UV-Vis. spectra and (B): photometric titrations of HBT-iodine charge transfer complex.

Photometric titration were performed at 25 °C for the reactions of HBT with iodine and picric acid in different solvents such as CHCl_3 and CH_3OH under the conditions of fixed HBT concentration (1.0×10^{-4} M) while the concentration of (iodine & picric acid) was changed over the range from 0.25×10^{-4} to 3.0×10^{-4} M and these produced solutions with HBT: I_2 and HBT:PA ratio varies from (1:0.25) to (1:3). These ratios were practically achieved by mixing 1 mL of HBT donor (5×10^{-4} M) with X mL of iodine and picric acid (5×10^{-4} M) and the mixture volume was diluted in each case to 5 mL by the use solvent. The electronic absorption spectra of the HBT donor, acceptors (iodine and picric acid) and the formed CT-complexes in chloroform and methanol were recorded in the region of 200-800 nm using UV-Vis. Spectrophotometer model Shimadzu UV-spectrophotometer model Jenway 6405 Spectrophotometer with quartz cell of 1.0 cm length. Photometric titrations were performed for the reactions between the acceptors (iodine and picric acid) and the HBT donor in chloroform and methanol at 25 °C. The concentrations of the donors in the reaction mixtures was kept fixed at (1×10^{-4} M) while the concentrations of iodine and picric acid was changed over the range from 0.25×10^{-4} to 4.0×10^{-4} M and these produced solutions with (HBT:acceptor) ratio varied from (1:0.25) to (1:4). These ratios were practically achieved by mixing 1 mL of HBT donor 5×10^{-4} M while X mL of acceptors (5×10^{-4} M) and each mixture volume was diluted in each case to 5 mL chloroform and methanol.

The concentration of HBT remained constant during these measurements, although the acceptors (iodine and picric acid) concentrations fluctuated between 0.25×10^{-4} M and 4.00×10^{-4} M, as detailed in the experimental section. Figures 1B and 2B display photometric titration curves derived from these results. The HBT-acceptors equivalence points show that the ratio is 1:1 in every situation, which is in good agreement with the solid CT-complexes elemental analysis and infrared spectra. The general formula of the CT-complexes that are generated when HBT reacts as a donor with the iodine and picric acid acceptors that are being studied in chloroform and methanol is [(HBT)(acceptor)]. The equilibrium constant, K, and the extinction coefficient, ϵ were determined using the 1:1 modified Benesi-Hildebrand equation (1) [41]. The initial concentrations C_a of the acceptors (iodine, and picric acid) and the initial concentration C_d of donor HBT are represented, while the absorbance of the strong bands around 510 nm for [(HBT)(I_2)], and 353 nm for [(HBT)(PA)] complexes were referred by A. For the reactions of HBT with iodine in

CHCl₃ and HBT with picric acid in methanol solvent, a straight line with a slope of 1/ε and an intercept of 1/Kε is generated by plotting the C_a+C_d values against C_a.C_d/A values for each acceptor. Table 1 provides the (K) and (ε) values for these complexes [(HBT)(I₂)] and [(HBT)(PA)].

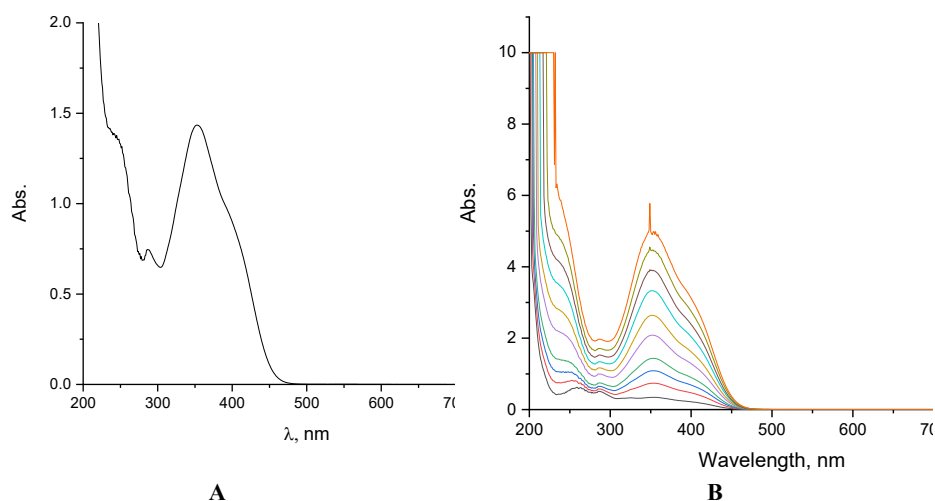


Figure 2. (A): UV-Vis. spectra and (B): photometric titrations of HBT-picric acid charge transfer complex.

Both the formation constant and the extinction coefficients exhibit large values in these charge transfer complexes. Because of the anticipated substantial donation of HBT, these high values of formation constant validate the predicted high stabilities of the generated CT-complexes. The type of acceptor employed, including the kind of substituents that drain electrons from it, like nitro groups, has a significant impact on the equilibrium constants. For instance, Table 1 shows that the equilibrium constant for [(HBT)(PA)] is larger than the equilibrium constant for the complex [(HBT)(I₂)], indicating that picric acid has a comparatively higher electron accepting ability.

$$\frac{C_a^o C_d^o l}{A} = \frac{1}{K\varepsilon} + \frac{C_a^o + C_d^o}{\varepsilon} \quad (1)$$

$$f = (4.319 \times 10^{-9}) \varepsilon_{\max} \cdot \nu_{1/2} \quad (2)$$

$$\mu \text{ (Debye)} = 0.0958 [\varepsilon_{\max} \nu_{1/2} / \nu_{\max}]^{1/2} \quad (3)$$

$$I_p \text{ (eV)} = 5.76 + 1.53 \times 10^{-4} \nu_{CT} \quad (4)$$

$$E_{CT} = (h\nu_{CT}) = 1243.667 / \lambda_{CT} \text{ (nm)} \quad (5)$$

$$\varepsilon_{\max} = 7.7 \times 10^4 / [h\nu_{CT} / [R_N] - 3.5] \quad (6)$$

$$\Delta G^{\circ} = -2.303 RT \log K_{CT} \quad (7)$$

Table 1. Spectrophotometric data of the HBT charge transfer complexes

λ_{\max} (nm)	E_{CT} (eV)	K (L.mol ⁻¹)	ϵ_{\max} (L.mol ⁻¹ .cm ⁻¹)	f	μ	I_p	R_N	$\Delta G^\circ(25^\circ\text{C})$ KJmol ⁻¹
[(HBT)(I ₂)] complex								
510	2.44	895	9960	5.06	23.42	8.76	0.217	16842
[(HBT)(PA)] complex								
353	3.52	425	358423	135	100	10.09	0.948	14999

Equation (3) has been used to compute the transition dipole moment (μ) of the HBT complexes (Table 1) [42], where ϵ_{\max} and ν_{\max} are the extinction coefficient and wavenumber at the maximum absorption peak of the CT complexes, respectively, and $\nu_{1/2}$ is the bandwidth at half-maximum of absorbance. Using the following formulas obtained by Aloisi and Piganatro [43, 44], the ionization potential (I_p) of the free HBT donor was calculated from the CT energies of the CT band of its complexes with various π -acceptors. The energy of the π - σ^* , n - σ^* , π - π^* , or n - π^* interaction (E_{CT}) is determined using Equation (5) [42], where λ_{CT} is the wavelength of the complexation band, and E_{CT} is the energy of the CT of the HBT complexes. The relationship shown in Equation (6), where ϵ_{\max} is the molar extinction coefficient at maximum CT absorption, ν_{CT} is the frequency of the CT peak, and R_N is the resonance energy of the complex in the ground state, was theoretically derived from Briegleb and Czekalla [45]. This relation is clearly a contributing factor to the stability constant of the complex (a ground state property). Table 1 lists the R_N values for the iodine and picric acid complexes that are being investigated. Equation (7) [46] was used to compute the standard free energy changes of complexation (ΔG°) from the association constants. Table 2 displays the calculated values, where ΔG° is the complex free energy change (KJ mol⁻¹), R is their gas constant (8.314 J mol⁻¹ K), T is their temperature in Kelvin degrees (273 + °C), and K_{CT} is their association constant (l mol⁻¹) in various solvents at room temperature. Exothermic feature reactions are the process by which HBT charge transfer complexes are formed, and the data of ΔG° has a negative value in accordance with the larger values of the formation constant.

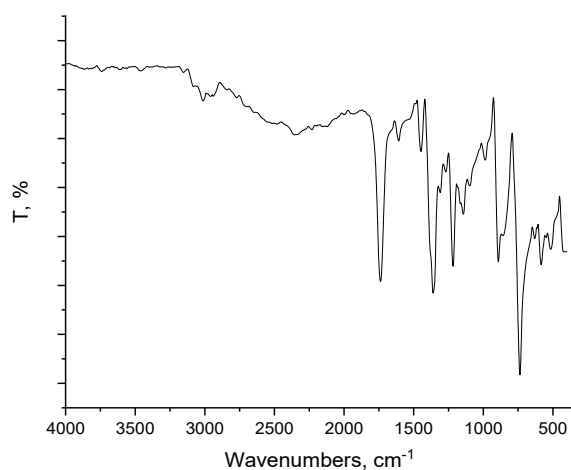
Infrared and Raman spectra

FTIR spectra of [(HBT)(I₂)] and [(HBT)(PA)] charge transfer complexes were scanned as KBr pellets within 4000–400 cm⁻¹ region (Figures 3 and 4). The infrared spectrum of free HBT donors shows no absorption band in the region of 1700–1650 cm⁻¹ (Table 2), which can be assigned to $\nu(\text{C}=\text{N})$ linkage. The stretching frequencies bands of the hydroxyl group of the hydroxy benzotriazole molecule $\nu(\text{O}-\text{H})$ absorption [47] are observed with strong intensity band at 3290 cm⁻¹. A band is present in the region of 1625–1600 cm⁻¹, that can be assigned to $\nu(\text{N}=\text{N})$ group. It has shown that the presence of $\nu(\text{N}=\text{N})$ vibrations at 1618 cm⁻¹ in HBT free ligand. In the free HBT donor, the C=C stretching absorption bands at 1552, 1490, 1477, and 1450 cm⁻¹ are due to aromaticity of benzene ring. The CH in-plane bending vibrations of for the aromatic HBT donor have some bands at around 1280–1235 cm⁻¹. The CH out-of-plane deformation characteristic vibrations bands of the aromatic benzene ring are at 991–742 cm⁻¹. The characteristic bands for the C–N bonds due to the triazole ring are at 1392, 1383, and 1309 cm⁻¹. The vibration due to the hydroxyl group appear at 1230–1180 cm⁻¹ region. Nakamoto [47] has shown $\nu(\text{N}-\text{OH})$ absorption at 1188 cm⁻¹. The characteristic vibration frequencies of the ring system in HBT have been observed in the region of 1552–640 cm⁻¹.

Table 2. Infrared frequencies (cm^{-1}) and band assignments of free HBT, [(HBT)(I₂)], and [(HBT)(PA)] charge transfer complexes.

Frequencies (cm^{-1})			Assignments
HBT	[(HBT)(I ₂)]	[(HBT)(PA)]	
3290, 3279	3010	3068	$\nu(\text{O-H})$
-	2700–2300	2700-2300	Hydrogen bonding
-	-	-	$\nu(\text{C=N})$
1618	1600	1605	$\nu(\text{N=N})$
1552, 1490, 1477, 1450	1446	1533, 1431	$\nu(\text{C=C})$
1392, 1383, 1309	1354	1329	$\nu(\text{C-N})$
1280, 1272, 1235	1217	1267, 1228	$\delta(\text{CH})$ in-plane bending
1188	1140	1150	$\nu(\text{N-OH})$
991, 975, 912, 903, 846, 783, 760, 742	1092, 985, 898, 733	889, 743, 700	$\delta(\text{CH})$ out-of-plane
-	-	583, 549, 501	$\delta(\text{NO}_2)$: PA

The FTIR spectra of [(HBT)(I₂)], and [(HBT)(PA)] charge transfer complexes show shifts to lower wavenumbers for the hydroxyl group from 3290 and 3279 cm^{-1} (free HBT) to 3010 and 3068 cm^{-1} , and the stretching vibration motion of $\nu(\text{N-OH})$ from 1188 cm^{-1} (free HBT) to 1140 and 1150 cm^{-1} in case of both HBT complexes. Also, the characteristic bands of benzotriazole moiety ($\nu(\text{N=N})$ and $\nu(\text{C-N})$) are shifted to lower wavenumbers from 1618 & 1392 cm^{-1} (free HBT) to 1605–1600 cm^{-1} and 1354–1329 cm^{-1} after charge transfer complexation. The shifted of –OH frequency in the spectra of the complexes indicate the complexation of iodine and picric acid acceptors through –OH group of HBT donor. The structures suggested of the charge transfer complexes formed between HBT-I₂ and HBT-PA are mentioned in formulas I and II. These data are well agreement with the infrared data which supported the place of charge-transfer complexation through the migration of protons (–OH of phenolic group of picric acid acceptor) from acidic centers to oxygen atom (hydroxyl group).



3A

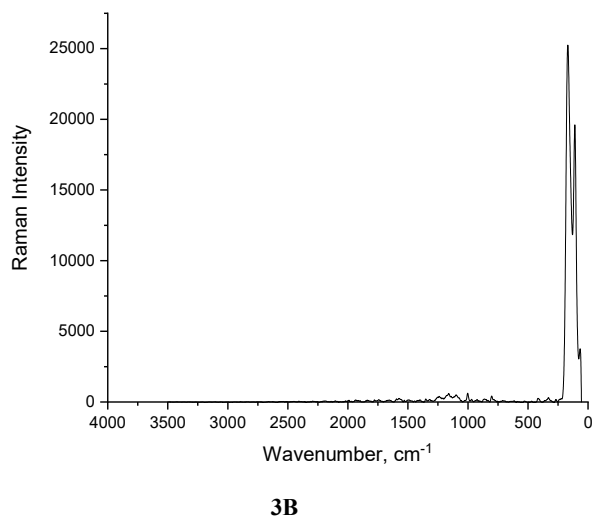


Figure 3. A: Infrared and B: Raman spectra of HBT-iodine charge transfer complex.

The Raman spectrum of the solid iodine, [(HBT)(I₂)], complex is shown in Figure 3 and its band assignments are comparable with symmetry data in literature survey [47]. The experimental data of this study recorded only two active Raman bands in the spectrum of the [(HBT)(I₂)] complex at 165 and 113 cm⁻¹ which matched with discrete iodine unit. The strong band at 165 cm⁻¹ is assigned to the $\nu_s(I-I)$ outer bonds, while the band at 113 cm⁻¹ is associated to the $\nu_s(I-I)$ inner bonds [47].

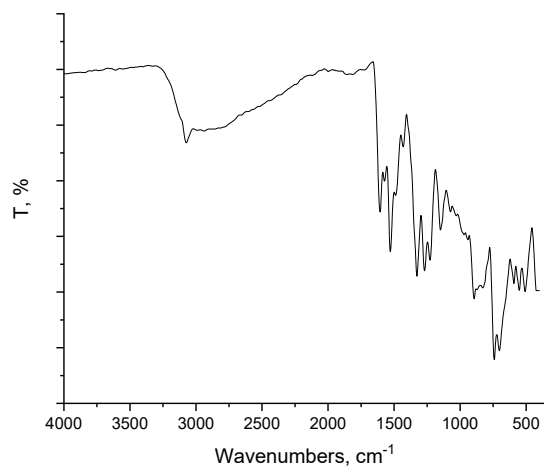


Figure 4. Infrared spectrum of HBT-picric acid charge transfer complex.

SEM and EDX investigations

Figures 5 and 7 display the recorded images from the scanning electron microscope (SEM) used to analyze the microstructural characteristics of the synthesized CT-complex. Figures 6 and 8 display the EDX spectrum of elemental analysis.

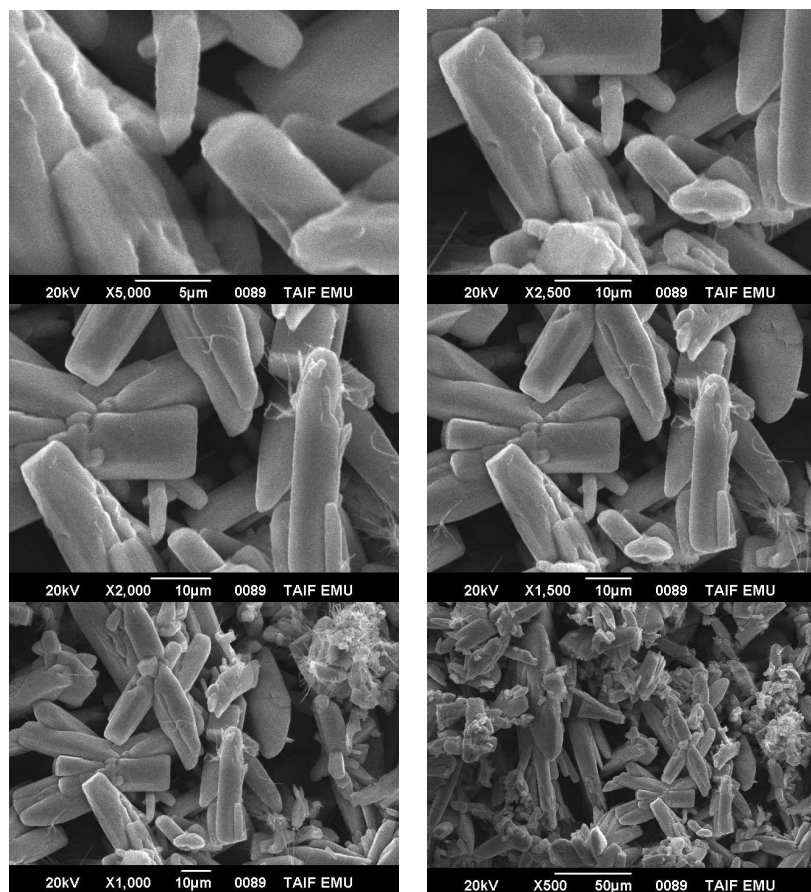


Figure 5. SEM images of HBT-iodine charge transfer complex with different magnifications (x5000, 2500, 2000, 1500, 1000, and 500).

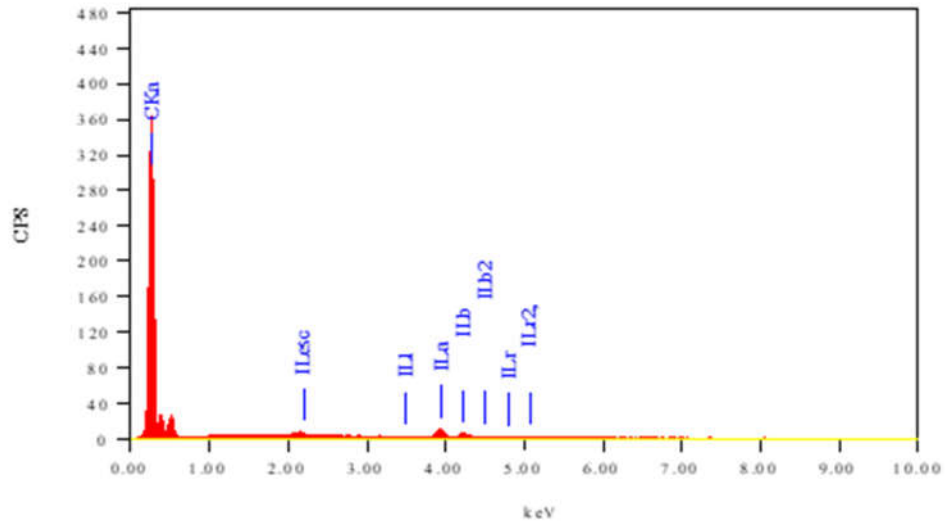
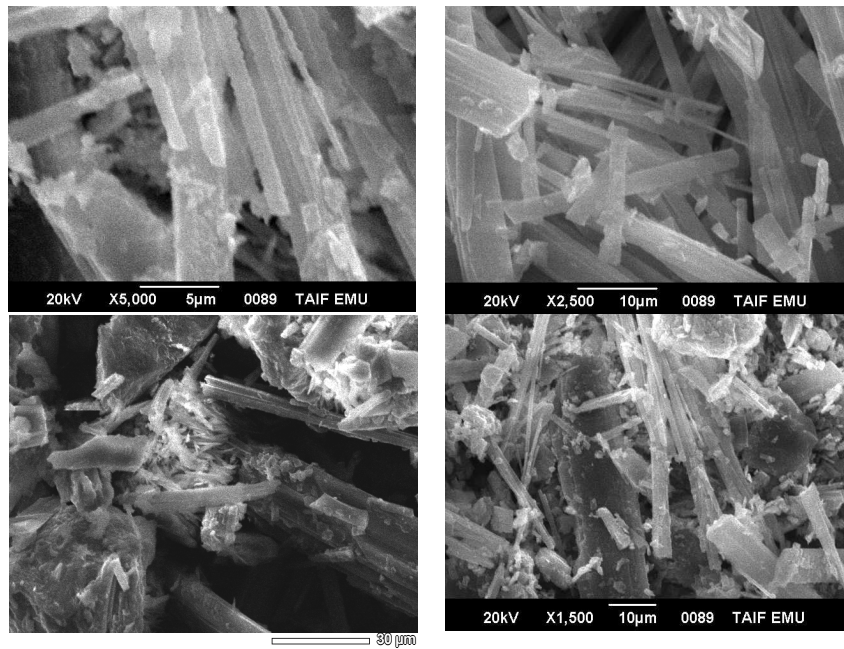


Figure 6. EDX spectrum of HBT-iodine charge transfer complex.



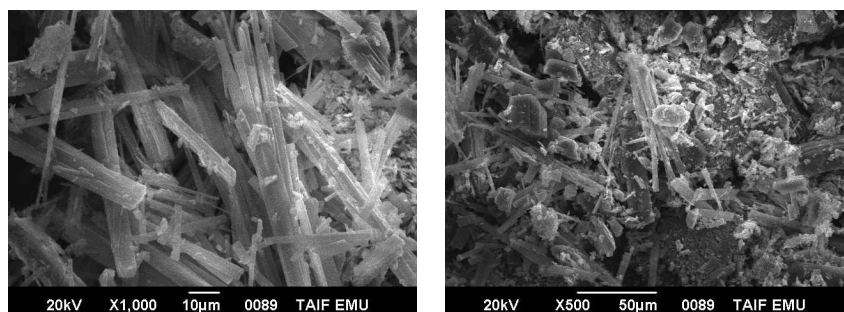


Figure 7. SEM images of HBT-picric acid charge transfer complex with different magnifications (x5000, 2500, 2000, 1500, 1000, and 500).

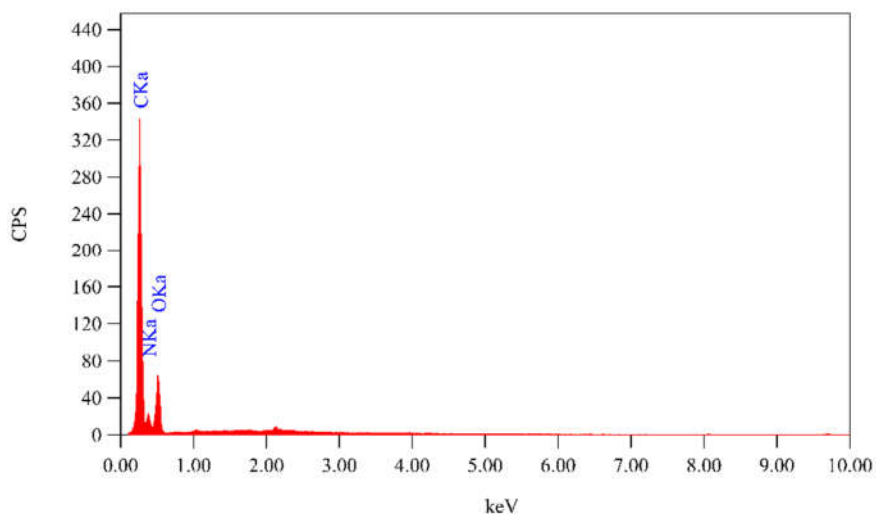


Figure 8. EDX spectrum of HBT-picric acid charge transfer complex.

The elemental composition and surface morphology of the CT complexes [HBT](I₂) and [HBT](PA) were investigated using energy dispersive X-ray (EDX) analysis and scanning electron microscopy (SEM). The relevant findings are displayed in Figures 5-8, where the SEM pictures reveal the goods' bars- and strips-shaped microstructures. The C, N, O, and I elemental peaks in the EDX spectra verified the compositions of the CT complexes formed with the donor and acceptors (Figures 6 and 8).

CONCLUSIONS

In chloroform and methanol solvents, a new charge transfer complexes between HBT as electron donor and (iodine and picric acid) as electron acceptors were investigated. The physical composition was confirmed to be 1:1 using photometric method. Spectroscopic physical parameters for the CT complex, such as ϵ_{CT} , K_{CT} , E_{CT} , R_N , I_p , μ and ΔG° were analyzed using the spectral data. The synthesized solid complexes were characterized by electronic UV-Vis and FT-IR spectra and it confirms the H-bonded CT complex. The surface shape as well as the elemental

analyses were both validated by the SEM-EDX spectra, and the structure appears to be of the bars- and strips-shaped type.

ACKNOWLEDGMENT

The authors would like to acknowledge Deanship of Graduate Studies and Scientific Research, Taif University for funding this work.

REFERENCES

1. McKellar, Q.A.; Scott, E.W. The benzimidazole anthelmintic agents a review. *J. Vet. Pharmacol. Ther.* **1990**, *13*, 223-247.
2. Barot, K.P.; Nikolova, S.; Ivanov, I.; Ghate, M.D. Novel research strategies of benzimidazole derivatives: a review. *Mini Rev. Med. Chem.* **2013**, *13*, 1421-1447.
3. Piccionello, A.P.; Guarcello, A. Bioactive compounds containing benzox adiazole, benzothiadiazole, benzotriazole. *Curr. Bioact. Compd.* **2010**, *6*, 266-283.
4. Suma, B.V.; Natesh, N.N.; Madhavan, V. Benzotriazole in medicinal chemistry: An overview. *J. Chem. Pharm. Res.* **2011**, *3*, 375-381.
5. Katritzky, A.R.; Rogovoy, B.V.; Chassaing, C.; Vvedensky, V. Di(benzotriazol-1-yl)methanimine: A new reagent for the synthesis of tri- and tetrasubstituted guanidines. *J. Org. Chem.* **2000**, *65*, 8080-8082.
6. Katritzky, A.R.; Rogovoy, V.; Vvedensky, V.Y.; Kovalenko, K.; Steel, P.J.; Markov, V.I.; Forood, B. Synthesis of N,N-disubstituted 3-amino-1,2,4 triazoles. *Synth.* **2001**, *6*, 897-903.
7. Katritzky, A.R.; Xie, L.; Toader, D.; Serdyuk, L. General and efficient carbon insertion route to one-carbon-homologated alpha-aryl, alpha-alkenyl, alpha-alkoxy, and alpha-phenylthio alkyl ketones. *J. Am. Chem. Soc.* **1995**, *117*, 12015-12016.
8. Boche, G.; Andrews, P.; Harms, K.; Marsch, M.; Rangappa, K.S.; Schimeczek, M.; Willeke, C. Crystal and electronic structure of stable nitrenium ions. A comparison with structurally related carbenes. *J. Am. Chem. Soc.* **1996**, *118*, 4925-4930.
9. Talukdar, S.; Chen, R.J.; Chen, C.T.; Lo, L.C.; Fang, J.M. Polymer-supported benzotriazoles as catalysts in the synthesis of tetrahydroquinolines by condensation of aldehydes with aromatic amines. *J. Comb. Chem.* **2001**, *3*, 341-345.
10. Davis, D. Benzotriazole, a plant-growth regulator. *Sci.* **1954**, *120*, 989.
11. Picci, V. Effect of benzotriazole and of 2 benzotriazolylacetic acids on plant growth. *Farm. Sci.* **1966**, *21*, 172-177.
12. Sparatore, F.; La Rotonda, M.I.; Paglietti, G.; Ramundo, E.; Silipo, C.; Vittoria, A. Benzotriazole derivatives active on plant growth. I. Preparation, characterization, and correlation between physicochemical properties and structure. *Farm. Sci.* **1978**, *33*, 901-923.
13. Sparatore, F.; La Rotonda, M.I.; Ramundo, E.; Silipo, C.; Vittoria, A. Effect of benzotriazole derivatives on plant growth. II. *Farm. Sci.* **1978**, *33*, 924-944.
14. Paglietti, G.; Sanna, P.; Carta, A.; Sparatore, F.; Vazzana, I.; Peana, A.; Satta, M. Choleric activity of 3-[ring substituted benzotriazol-1(2)-yl]alkanoic and alkenoic acids. *Farm. Sci.* **1994**, *40*, 693-702.
15. Jamkhandi, C.M.; Disouza, J.I. Benzotriazole derivatives as antimicrobial agents. *Asian J. Pharm. Biol. Res.* **2012**, *2*, 123-130.
16. Lopez-Vallejo, F.; Castillo, R.; Yopez-Mulia, L.; Medina-Franco, J.L.; Benzotriazoles and indazoles are scaffolds with biological activity against *Entamoeba histolytica*. *J. Biomol. Screen.* **2011**, *16*, 862-868.
17. Borowski, P.; Deinert, J.; Schalinski, S.; Bretner, M.; Ginalski, K.; Kulikowski, T.; Shugar, D. Halogenated benzimidazoles and benzotriazoles as inhibitors of the NTPase/helicase activities of hepatitis C and related viruses. *Eur. J. Biochem.* **2003**, *270*, 1645-1653.

18. Beauchard, A.; Jaunet, A.; Murillo, L.; Baldeyrou, B.; Lansiaux, A.; Cherouvrier, J.R.; Domon, L.; Picot, L.; Bailly, C.; Besson, T.; Thiery, V. Synthesis and antitumoral activity of novel thiazolobenzotriazole, thiazoloindolo[3,2-c]quinoline and quinolinoquinoline derivatives. *Eur. J. Med. Chem.* **2009**, *44*, 3858-3865.
19. Altalhi, T.; Gobouri, A.A.; Refat, M.S.; El-Nahass, M.M.; Hassanien, A.M.; Atta, A.A.; Al Otaibi, S.; Kamal, A.M. Optical spectroscopic studies on poly(methylmethacrylate) doped by charge transfer complex. *Opt. Mat.* **2021**, *117*, 111152.
20. Usmana, R.; Khan, A.; Tang, H.; Ma, D.; Alsuhaibani, A.M.; Refat, M.S.; Adnan, Ara, N.; Fan, H.-J.S. Charge transfer and hydrogen bonding motifs in organic cocrystals derived from aromatic diamines and TCNB. *J. Mol. Struct.* **2022**, *1254*, 132360.
21. Alrooqi, A.; Al-Amshany, Z.M.; Al-Harbi, L.M.; Altalhi, T.A.; Refat, M.S.; Hassanien, A.M.; Atta, A.A. Impact of charge transfer complexes on the dielectric relaxation processes in poly(methyl methacrylate) polymer. *Mol.* **2022**, *27*, 1993.
22. Alkathiri, A.A.; Atta, A.A.; Refat, M.S.; Altalhi, T.A.; Shakya, S.; Alsawat, M.; Adam, A.M.A.; Mersal, G.A.M.; Hassanien, A.M. Preparation, spectroscopic, cyclic voltammetry and DFT/TD-DFT studies on fluorescein charge transfer complex for photonic applications. *Bull. Chem. Soc. Ethiop.* **2023**, *37*, 515-532.
23. Alsuhaibani, A.M.; Refat, M.S.; Islam, M. Biological and computational exploration of a hydrogen-bonded charge transfer complex between 8-hydroxyquinoline and benzene-1,4-diol in different polar solvents: Synthesis and spectrophotometric analysis. *J. Mol. Struct.* **2025**, *1319*, 139440.
24. Al-Humaidi, J.Y.; El-Sayed, M.Y.; Refat, M.S.; Altalhi, T.A.; Eldaroti, H.H. Spectrophotometric studies on the charge transfer interactions between thiazolidine as a donor and three π -acceptors: *p*-chloranil (CHL), DDQ and TCNQ. *J. Mol. Liq.* **2021**, *333*, 115928.
25. Karmakar, A.; Singh, B. Charge-transfer interaction of 4-(2-pyridylazo) resorcinol with nitroaromatics: insights from experimental and theoretical results. *J. Mol. Liq.* **2017**, *236*, 135-143.
26. Karmakar, A.; Kundu, K.; Ghosh, S.; Mukhopadhyay, C.; Nayek, S.K.; Chaudhuri, T. Recognition of steric factor in external association of xanthenocrown-5 and bis-naphthalenocrown-6 with bis (benzimidazolium) propane borontetrafluoride. *Spectrochim. Acta A* **2016**, *159*, 141-145.
27. Chaudhuri, T.; Shivran, N.; Mula, S. Bodipy recognizes polyaromatic hydrocarbons via C-H... F type weak H-bonding. *RSC Adv.* **2016**, *6*, 59237-59241.
28. Alanazi, A.; Abounassif, M.; AlRabiah, H.; Mostafa, G.A.E. Development of two charge transfer complex spectrophotometric methods for determination of tofisopam in tablet dosage form. *Trop. J. Pharm. Res.* **2016**, *15*, 995-1001.
29. Al-Badr, A.; Mostafa, G.A.E. Spectrophotometric determination of trimipramine in tablet dosage form via charge transfer complex formation. *Trop. J. Pharm. Res.* **2013**, *12*, 1057-1063.
30. Kololkovas, A. *Essentials of Medicinal Chemistry*, 2nd ed., Wiley: New York; **1998**.
31. Mandal, R.; Lahiri, S.C. Interactions of L-amino acids with metronidazole and tinidazole. *J Indian Chem. Soc.* **1999**, *76*, 347-349.
32. Refat, M.S.; Ibrahim, O.B.; Saad, H.A.; Adam, A.M.A. Usefulness of charge-transfer complexation for the assessment of sympathomimetic drugs: Spectroscopic properties of drug ephedrine hydrochloride complexed with some π -acceptors. *J. Mol. Struct.* **2014**, *1064*, 58-69.
33. Eldaroti, H.H.; Gadir, S.A.; Refat, M.S.; Adam, A.M.A. Spectroscopic investigations of the charge-transfer interaction between the drug reserpine and different acceptors: Towards understanding of drug-receptor mechanism. *Spectrochim. Acta A* **2013**, *115*, 309-323.
34. Adam, A.M.A.; Refat, M.S.; Saad, H.A. Spectral, thermal, XRD and SEM studies of charge-transfer complexation of hexamethylenediamine and three types of acceptors: π -, σ - and

- vacant *orbital* acceptors that include quinol, picric acid, bromine, iodine, SnCl₄ and ZnCl₂ acceptors. *J. Mol. Strut.* **2013**, 1051, 144-163.
35. Adam, A.M.A.; Refat, M.S.; Saad, H.A. Utilization of charge-transfer complexation for the detection of carcinogenic substances in foods: Spectroscopic characterization of ethyl carbamate with some traditional π -acceptors. *J. Mol. Strut.* **2013**, 1037, 376-392.
 36. Andrews, L.; Prochaska, E.S.; Loewenschuss, A. Resonance Raman and ultraviolet absorption spectra of the triiodide ion produced by alkali iodide-iodine argon matrix reactions. *Inorg. Chem.* **1980**, 19, 463-465.
 37. Ikemoto, I.; Sakairi, M.; Tsutsumi, T.; Kuroda, H.; Harada, I.; Tasumi, M.; Shirakawa, H.; Ikeda, S. X-ray photoelectron spectroscopic study of highly conductive iodine-doped polyacetylene. *Chem. Lett.* **1979**, 1189-1192.
 38. Rajpure, K.Y.; Bhosale, C.H. Sb₂S₃ semiconductor-septum rechargeable storage cell. *Chem. Mater. Chem. Phys.* **2000**, 64, 70-74.
 39. Licht, S. Electrolyte modified photoelectrochemical solar cells. *Sol. Energy Mater. Sol. Cells* **1995**, 38, 305-319.
 40. Refat, M.S.; El-Didamony, A.; Grabchev, I. UV-vis, IR spectra and thermal studies of charge transfer complex formed between poly(amidoamine) dendrimers and iodine. *Spectrochim. Acta Part A* **2007**, 67, 58-65.
 41. Skoog, D.A. *Principle of Instrumental Analysis*, 3rd ed., Saunders College Publishing: New York; **1985**; Ch. 7.
 42. Rathone, R.; Lindeman, S.V.; Kochi, J.K. Charge-transfer probes for molecular recognition *via* steric hindrance in donor-acceptor pairs. *J. Am. Chem. Soc.* **1997**, 119, 9393-9404.
 43. Briegleb, G. Z. Electron affinity of organic molecules. *Angew. Chem.* **1964**, 3, 317-632.
 44. Aloisi, G.; Pignataro, S. Molecular complexes of substituted thiophens with σ and π acceptors. Charge transfer spectra and ionization potentials of the donors. *J. Chem. Soc. Faraday Trans.* **1972**, 69, 534-539.
 45. Briegleb, G.; Czekalla, J. Intensity of electron transition bands in electron donator-acceptor complexes. *Z. Physikchem. (Frankfurt)*. **1960**, 24, 37-54.
 46. Martin, A.N.; Swarbrick, J.; Cammarata, A. *Physical Pharmacy*, 3rd ed., Lee and Febiger: Philadelphia, PA; **1969**; pp. 344.
 47. Nakamoto, K. *Infrared and Raman Spectra of Inorganic and Coordination Compounds*, Wiley: New York; **1978**.